

# Particle size and abundance measurements suggest temporally variable biotic transport and disaggregation in the Eastern Tropical North Pacific Oxygen Minimum Zone

Jacob A. Cram

07 January 2020

## Author list

(putative, order not set, please suggest others, will likely expand) Jacob Cram, Jessica Pretty, Megan Duffy, Rachael L, Clara Fuchsman, Klaus H, Thomas Weber, Shirley Leung, Jaqui N, Allan Duvol, Rick Keil, Andrew McDonnel

## Abstract

Models and observations suggest that particle flux attenuation is lower across the mesopelagic zone of anoxic environments compared to oxic ones. This attenuation is likely a function of microbial metabolism, as well as aggregation and disaggregation by zooplankton. Analysis of particle size spectra provide insight into the relative roles of aggregation, disaggregation and remineralization. We measured particle size profiles at one station in the core of the Eastern Tropical North Pacific Oxygen Minimum Zone (ETNP OMZ) using an underwater vision profiler (UVP), at different times of day, over the course of a week. We normalized our UVP measurements by comparing them to particle flux measurements measured by sediment traps. We also explored how our measurements related to acoustic observations of migratory marine species. We compared our observations to UVP measurements from a site at the same latitude but different longitude, where oxygen concentrations were non-limiting.

Particle numbers remain constant through 500m and then decrease through 1000m. Particle size distribution slopes steepen until 500m, suggesting a higher proportion of small particles, flatten below 500m, and then steepen again below the OMZ. Particle flux at our site was characterized by rapid attenuation in the top layer of the OMZ followed by either low attenuation or a small increase in abundance, depending on the day of the study and hour of the day in the core of the OMZ, a region to which plankton of a range of sizes migrated during the day. These patterns suggest slower attenuation of particles of all sizes, rather than decreased disaggregation of particles, or slower attenuation of just large particles is responsible for the lower flux attenuation in this region. A model of particle remineralization and shrinking was used to diagnose whether particle size patterns violated the assumption that particles only sink and remineralize, and are neither aggregated, disaggregated, or transported by zooplankton. Our model suggested the presence of disaggregation like processes between 250 and 500m of in the water column that occurred at all time-points. Our data suggest a role of zooplankton in transporting biomass in the form of fecal pellets, into the core of the OMZ, but also in disaggregating particles in this same region. We further observe that there is temporal variability in flux transport.

# Introduction

- A
  - The biological pump is a key part of the global carbon cycle in which, sinking particles transport carbon from the surface into the deep ocean. (Turner 2015; Neuer 2014) (Neuer, Iversen, and Fischer 2014; Turner 2015).
  - Flux into the deep ocean is a function of both export from the photic zone into the mesopelegic (export flux), and the fraction of that flux that crosses the mesopelegic (transfer efficiency) (Ref).
  - Much has been said about particle dynamics in the surface and their relation to export flux (Jackson and Burd; Jokulsdottir; Kriest; Others)
  - Transfer efficiency, the flux between the base of the photic zone and the deep ocean (Francois 2002) (Francois et al. 2002) is important in particular, because the depth to which carbon is transported may affect global atmospheric carbon levels (Kwon) (Kwon, Primeau, and Sarmiento 2009)
  - Zooplankton can affect particle flux in the mesopelegic in several ways (Turner 2015; Steinberg and Landry 2017)(Steinberg and Landry 2017; Turner 2015), and by extension the efficiency of the biological pump (Cavan 2017)(Cavan et al. 2017).
    - \* (1) They repackage particles into fecal pellets which have different properties from the original particles Steinberg and Landry – and refs therein)
    - \* (2) They consuming particles in surface depths and releasing at others zooplankton actively transport carbon (usually downward) (Steinberg et al., 2000; Hannides et al., 2009; Bianchi et al., 2013; Stukel et al., 2018b; Archibald et al., 2019; {<- All from stukel et al 2019}, Kiko recent).
    - \* (3) Zooplankton may consume particles in the mesopelegic and respire much of their biomass (Stukel et al. 2019)
    - \* (4) Zooplankton may break large particles into smaller ones, through sloppy feeding (Cavin)(Cavan et al. 2017), or by generating turbulence that breaks down particles (in Turner 2015 -> Goldthwait et al. 2004)(Goldthwait et al. 2004), or part of a complex “gardening” (Mayor et al. 2014)(Mayor 2014).
  - Fragmentation of particles can lead to increased remineralization of particles because those smaller particle pieces sink more slowly and so have longer residence times, and so have longer to break down in the mesopelegic (Goldthwait et al. 2005).
  - Oxygen levels, and in particular anoxic regions of the water column, appear to modulate particle flux through the mesopelegic
    - \* Evidence
      - Models (Cram, Devries and Weber, Bianchi and Weber)
      - Observations: Arabian Sea (Keil, Neibauer, and Devol 2016) (Kiel et al 2016). ETNP, closer to coast (Van Mooy, Keil, and Devol 2002) (Van Mooy et al. 2002).
    - \* This is important because oxygen minimum zones are expanding, and understanding their influence on ocean biogeochemistry is critical for understanding future oceans.
    - \* Pelagic oxygen minimum zones are expanding(Stramma et al. 2008), and this expansion is likely to effect ocean chemistry, the habitat of marine organisms, and the interactions between between organisms and chemistry (Gilly et al. 2013). Models and chemical data suggest that oxygen minimum zones may enhance carbon transport to the deep ocean, by inhibiting microbial degradation of sinking marine particles (Cram et al. 2018). However, biological organic matter transport is modulated by zooplankton (Steinberg et al. 2008; Steinberg and Landry 2017) which feed on, produce and disaggregate particles, and whose interactions on particle flux in pelagic OMZs are only beginning to be explored (Kiko et al. 2020).
  - Particle size resolved models of TEFF in the oceans suggest that temperature, size and oxygen play a big role. (Cram et al.; Weber and DeVries)
    - \* And regional differences in particle ballast plays a smaller role. (Cram et al.) -These models assume that zooplankton play a small role, and therefore assume no transport through the mesopelegic, and no disaggregation. -They therefore predict attenuation of small particles and not large ones.
    - \* A questionable assumption, given the established importance of zooplankton.

- \* However, These models particle size predictions generate a useful null hypothesis that can be compared against.
- Particle data provide valuable information about particle transport.
  - \* When performed in concert with traps, they can be used to predict flux in places where traps aren't (Guidi et al. 2008). They can give resolved information about particle flux variability across space and time (Guidi et al. 2008; Kiko et al. 2017).
  - \* They can tell us about the relationship between particle size and sinking speed (Guidi et al. 2008). (Guidi)
- A recent modeling study posed three hypotheses, each with a prediction about particle size distributions (Weber and Bianchi 2020) (Bianchi and Weber)
  - \* Bianchi and Weber (2020) proposed three reasons that this could occur
    - (1) Slower attenuation of *all* particles: The rate of generalization of all particles could be slower in OMZs.
    - (2) Decreased disaggregation by zooplankton:
    - (3) Slower attenuation of large particles: Large particles might harbor cores that are limited in both oxygen and nitrate and so microbial metabolism could be usually slow in these.
  - \* The authors proposed that these processes would have signature effects on particle size distribution in the core of the ETNP. Slower attenuation of all particles, was predicted to result in an increase in the abundance of small particles, while the other two models, would result in a decrease in small particle abundance as small particles were either not replaced by breakdown of large particles (Model 2) or as those particles were broken down more quickly than larger particles (Model 3). However, they didn't have data to determine which model best fit reality.
- A recent study combined particle size tracking, mockness tows, acoustic data, and trap measurements from the literature to explore zooplankton transport in a weak OMZ (Kiko et al. 2020).
  - \* They found a particle maximum and contended that it suggests transport by zooplankton, and mortality of migrating zooplankton.
  - \* They also suggested that in stronger and larger OMZs there might be less flux into the mesopelegic.
- B
  - Previous analyses of particles don't look directly at the particle size distribution slope.
  - TEFF models currently do not do a good job of predicting observed particle numbers
  - There isn't much data about particle size throughout the ETNP OMZ.
    - \* There isn't much data from oligotrophic, but very anoxic OMZs in general.
  - There isn't much resolved temporal data, which makes it hard to deconvolve ongoing processes from temporal variability in particle production at the surface.
  - Only one study to our knowledge combined measurements of traps, particles and acoustic data together
    - \* and none have traps at exactly the same time as the particle data.
  - The data to test the Bianchi-Weber models didn't previously exist.
  - Nobody has compared predictions of models to observed particle flux, and how those vary through the water column.
  - Most OMZ are in the oligotrophic ocean, where productivity is low (REFs from Clara). But most flux data has been measured in higher productivity regions (Van Mooy 2001)
- T
  - We targeted a site typical of the oligotrophic ETNP OMZ, well away from the high productivity zone in the coast.
  - We collected particle size data at high temporal resolution over a week
  - We compare it to observed flux measurements, and acoustic data.
  - We describe particle size distribution slope.
  - We test the Bianchi-Weber models.
  - We quantify, throughout the water column, how changes in size distribution deviate from changes that would be predicted by remineralization and sinking only models.

- Together, these analyses will provide more detailed information about the relationship between particle transport and zooplankton in the ETNP OMZ.

## **Scientific questions:**

- How do the particle size distribution at one location in the oligotrophic Eastern Tropical North Pacific evolve with respect to depth, and how does it vary over time?
- Do our data support any of the Bianchi-Weber models?
- Do our data suggest regions of the oxygen minimum zone with disaggregation like processes, and if so do these co-occur with regions suggested to harbor zooplankton.

## **We hypothesized**

- Temporal day to day variability in particle number, particles size distribution slope and flux would be evident.
- This variability would relate to the location of migratory zooplankton, with a combination of increased particle flux and disaggregation present where zooplankton occur.
- Disaggregation and particle production by zooplankton might lead to particle size patterns that cannot be explained by remineralization and sinking alone.
- All three of the Weber-Bianchi hypotheses.

## **Methods**

Unless specified otherwise, measurements were taken on board the R/V Sikuliaq from 07 January 2017 through 13 January 2017 at 16.5°N 106.9°W, located in an oligotrophic region of the Eastern Tropical North Pacific Oxygen Minimum Zone (Figure 1A). Data are compared against measurements taken at 16.5°N 152.0°W on 08 May. A same latitude region west of the OMZ, where oxygen is not limiting (Figure S1).

### **Water property measurement**

We measured water properties of temperature, salinity, fluorescence, oxygen concentration and turbidity using the shipboard XXX CTD {get sensor information}. Data were processed using seabird software and analyzed and visualized in *R*.

### **Particle size measurements**

Particle size data were collected by Underwater Vision Profiler 5 (UVP) that was mounted below the CTD-rosette and deployed for all CTD casts shallower than 2500 m. A UVP is a combination camera and light source that describes the abundance and size of particles from 100 microns to several centimeters in size (Picheral et al. 2010). Particles have been previously shown to be primarily “marine snow” but may also include a small number of zooplankton and visual artifacts. UVP data were processed using custom Matlab scripts, uploaded to EcoTaxa, and analyzed in *R*.

### **Flux measurements**

Particles were collected in incubating particle traps ({Someone in Ricks’ lab – what is a good reference for these?}). Traps were used to perform incubation studies which will be reported elsewhere. As part of these studies, the traps also generated data about carbon flux, which is reported here. Two types of traps were

deployed. The particles were collected in two kinds of traps. One set of traps, generally deployed in shallower water had a solid cone opening with a cone opening with area  $0.46 \text{ m}^2$ . The second set had larger conical net with opening of  $1.23 \text{ m}^2$  area made of 200 micron nylon mesh . In all cases particles collected in the net or cone fell into one of two chambers. The “plus-particles” chamber collected particles from the net and incubated them for an amount of time that ranged from X to X days. The top-collector trap collected particles, and then returned immediately to the surface. We preferentially used data from the “top-collector”; however in many cases, data was only available from the “plus-particles” trap, in which case we used that data.

## Analysis

All analyses were constrained to the mesopelegic, defined here as the region between the base of the photic zone and 1000m. For many analyses particles were binned by depth with 20 m resolution between the surface and 100m, 25 m resolution between 100m and 200 m depths and 50m resolution between 200m and 1000m. To perform this binning, particle numbers, and volumes of water sampled of each observation in the depth region were summed prior to other analyses.

Two normalized values of particle numbers were calculated. In the first, particle numbers were divided to volume sampled, to generate values in particles/ $\text{m}^3$ . In the second, particles were divided by both volume sampled and the width of the size bin by which particles were classed to generate values in particles/ $\text{m}^3/\text{mm}$ .

### Particle size distribution

We determined the slope and intercept of the particle size distribution spectrum by fitting a power law to the data. Because large particles were infrequently detected we used a negative-binomial-general linear model that considered the volume of particles sampled, and particle bin-size and that assumed that the residuals of the data followed a negative-binomial (rather than normal) distribution. Thus we fit the equation  $\log\left(\frac{\text{E(Total Particles)}}{\text{Volume} * \text{Binsize}}\right) = b_0 + b_1(\text{Size})$  to solve for the Intercept ( $b_0$ ) and particle size distribution slope ( $PSD = b_1$ ). Where the term on the left describes the expected volume and bin-size normalized count data, assuming a negative binomial distribution of residuals.

### Estimating particle flux

We estimated particle flux throughout the water column, by fitting particle data to observed trap data. We assumed that particle flux in each size bin (j) followed the equation

$$\text{flux}_j = \left( \frac{\text{Total Particles}_j}{\text{Volume} * \text{Binsize}_i} \right) * C_f * (\text{Size})^a$$

(Eqn 1.)

And where flux at a given depth is the sum of all bin specific values.

$$\text{Flux} = \sum_j \text{flux}_j$$

(Eqn 2.)

We used the `optimize()` function R’s `stats` package to find the values of  $C_f$  and  $a$  that yielded closest fits of the UVP estimated flux to each particle trap.

Assuming a spherical particle drag profile, it is possible to also derive the exponent of the particle size to biomass exponent  $\alpha$  and size to sinking speed exponent  $\gamma$  as described in the equations  $\text{Biomass}_j \sim \text{Size}_j^\alpha$  and  $\text{Speed}_j \sim \text{Size}_j^\gamma$  (Guidi et al. 2008), following the equations  $a = /alpha + /gamma$  and  $\gamma = \alpha - 1$ .

## Size specific information

We separately analyzed total particle numbers, particle size distribution, and particle flux for particles larger than or equal to 500 microns, and those smaller than 500 microns, to determine the relative contributions of these two particle classes to particle properties.

## Variability

We used a general additive model, of form  $Flux = s(Depth) + s(Day) + s(Hour)$  to explore whether estimated flux levels appeared to vary by day and hour, holding the effects of depth constant, in the 250 m to 500 m region. The smooth terms  $s$  for “Depth” and “Day” were thin plate splines, while the term for “Hour” was a cyclic spline of 24 hour period.

## Modeling remineralization and sinking

We modified the Particle Remineralization and Sinking (PRISM) model, as described by DeVries et al. (2014) to estimate particle size distributions at each depth in the water column from (1) the particle size distribution in the depth bin above, and (2) the estimated change in flux between the two depths (which is itself calculated from the two observed distributions) (Supplement). The model generates a predicted profile at the deeper depth, which can be compared to the shallower depth.

## Results

### Physical and Chemical Data

The anoxic zone, characterized by undetectable oxygen levels, extends from 80 m to 850 m depth, with a sharp upper oxycline and a gradual lower oxycline (Figure 1B-D). The upper oxycline tracks a sharp pycnocline (Figure 1C 1D), characterized by a abrupt drop in temperature below the mixed layer, and an increase in salinity (Figure 1B). The site is characterized two fluorescence maxima (Figure 1C). The larger, shallower fluorescence peak is positioned just above the oxycline, ending exactly where oxygen reaches zero. The smaller, lower peak is positioned entirely inside of the anoxic zone. Turbidity tracks the two chlorophyll peaks in the surface, and has a tertiary maximum at the lower oxycline (Figure 1D).

### Acoustic data reveal diel migration patterns

Acoustic data, produced by the shipboard EK60 , suggest the presence of multiple cohorts of migratory organisms. The largest organisms, observed by backscattering of the EK60’s 18000 Hz signal, showed the clearest patterns. Most migratory organisms appeared to leave the surface at dawn and return at dusk, spending the day between 250 and 500m (Figure 2A). There appeared to be two local maxima in backscattering intensity at mid-day, one at ~300m and one at ~375 m (Figure 2A). There also appeared to be organisms that migrated downward at dusk and upward at dawn , spending the night at ~300m (Figure 2B). There was also a peak of organisms that appeared, at mid-day, on some but not all days, without any visible dawn or dusk migration just above the base of the photic zone. (Figure 2C). Other characteristics included what appeared to be diel migrants that crossed the OMZ and spent the day below the range of the EK60 (Figure 2D), as well as organisms that appeared between 500m and 1000m but did not appear to migrate to or from that depth at our site, but rather simply transited through the the EK60’s field of view at that time (Figure 2D).

Similar patterns were evident each other measured frequency, with better resolution by the lower frequencies (Figure S2).

## Flux data from traps

Flux measurements at station P2 were consistent between the different particle trap types and chambers measured, and showed a profile that broadly represented a power law with respect to depth, with the exception that flux appeared to increase in one trap at 500m. Four traps in the surface had anomalously low measurements of flux, compared to similar traps placed at similar depths, which may have been due to trap malfunctions {Talk to Jaqui about these} (Figure 3).

## Particle abundance measurements vary with size and depth

In all profiles, particle abundances were highest at the surface, and highest among the smallest particles (Figure S3). Visual examination of the relationship between particle number and size suggested a power law relationship where the log of volume and bin-sized normalized particle abundance was proportional to the log of the particles size (Figure S4). The exception to this pattern was very large particles, which are rare enough that they are usually not detected by the UVP. Generalized linear models that assume a negative binomial distribution of the data were able to account for this under-sampling of large particles estimate power log slopes, while taking into account rare occurrences of the data, at each depth (Figure S4).

Total particle numbers were generally similar between different casts, regardless of which day or hour they were collected (Figure S5A). Particle numbers were highest in the surface and decreased rapidly, flattened out over the 250 m to 500m range, decreased again until the lower oxycline, and then increased below the oxycline (Figure S5A).

The particle size distribution slope steepened (became more negative) between the surface and 500m, flattened (became less negative) between 500m and 1000m, and then steepened again after 1000m (Figure S5B). Steeper, more negative, slopes indicate a higher proportion of small particles relative to large particles, while flatter, less negative, slopes indicate a higher proportion of large particles relative to other places.

## Estimated particle flux sometimes increases with depth in the OMZ core

Using an optimization algorithm, we found that there was greatest agreement between estimates of trap observed particle flux, and UVP estimated particle flux when the particle size to flux relationship was governed by the ratio

$$Flux = 133 * Size^{2.00}$$

. This resulted in a UVP predicted flux profile that broadly fit the expected trap observed flux profiles, excluding the four traps that were held out from the analysis due to low abundance.

Particle flux profiles varied notably between casts between the base the photic zone and 100 and 500m m (Figure 4a-b). Between 250 m and 500 m particle flux appeared to increase on some but not all casts, while attenuating slowly on others (Figure 4c). Below 500m, there were not enough casts to measure variability between casts.

General additive models that examined the rate of change of flux between 250 and 500m found that, after removing the effect of depth, there was a statistically significant relationship between day of the week and the fifth-root transformed, rate of change of flux ( $P = 0.002$ ), as well as between hour of the day and flux ( $P = 0.040$ ) (Figure S6). There were increases in flux over this region towards the beginning and end of the sampling period, and lowest near day 10. There was also increases in flux in the daytime but decreases at night-time. By comparing three general additive models, one that considered only depth, one that considered depth and day of the week and one that considered depth, day of week, and time of day, we found that while depth accounted for 37% of the variance, adding day of the week accounted for an additional 18% of the variance, and hour of the day accounted for only 8.7% of the remaining variance in transformed rate of change of flux. If the fifth root transformation was not applied to the rate of change of flux, the hourly pattern was not evident. Increases in flux in this region were clearly not limited to the daytime, as one midnight cast showed increases here as well (Figure 4C).

## ETNP particle dynamics differ from those seen at an oxic site

### Oxic Region: Chemistry

The oxic site was characterized by a more gradually sloping picnocline, and an oxygen minimum at 500m of  $19.7 \mu\text{M}$ , which is not anoxic (Figure S1B). The photic zone is characterized by a single fluorescence peak with a maximum at 110m and which disappeared at 200m (Figure S1C). Turbidity followed chlorophyll concentration and did not have a peak in the mesopelegic (Figure S1D), unlike the ETNP site. There was a salinity peak at 150m (Figure S1B).

### Anoxic Vs. Oxic Region: Particle Number and Size

Particle numbers were higher, between the base of the photic zone through 1000m at the ETNP site, than at the same-latitude, oxygenic P16 station 100 (Figure S7A). Particle size distributions were similar between the two sites above 500m, being characterized by overlapping confidence intervals generated by a general additive model. From 500 to 1000m, particle size distributions were steeper at the ETNP site, being characterized by a higher proportion of small particles (Figure S7B).

### Anoxic Vs.Oxic Region: Large vs small particles

Small particles ( $100 \mu\text{m} - 500 \mu\text{m}$ ) at the ETNP site were about two orders of magnitude more common than large particles ( $\geq 500 \mu\text{m}$ ) (Figure S8). Large particle numbers appeared to attenuate more quickly than small particles, and more generally follow a power law decrease, while small particles appeared to increase around 500 m. Flux was predicted to be predominantly from small, rather than large particles, at all depths except the very surface. The particle size distribution, calculated only on large particles, was more variable between depths than calculated for small particles. Data from the oxic P16 station 100 suggested more particles, steeper particle size distribution, and more flux than at this station than at the ETNP station. They also suggested that differences between large and small particles, with respect to number, flux and size distribution that were broadly similar to the ones seen at ETNP Station P2.

### Anoxic vs Oxic Flux

In contrast to the anoxic station, at the oxic station, flux always decreased with depth (Figure S9A+B).

### Smoothed and averaged data

Highly smoothed particle data suggested that particle size, averaged across all casts, followed a pattern in which the abundance of small particles increased in the OMZ surface (Figure 5A), which corresponded with characterized by steepening of the particle size distribution (Figure 5A), an increase in small particle biomass (Figure 5B), but not of large particle biomass (Figure 5C). Deeper in the OMZ the small particle number, PSD slope, and biomass of small particles declined.

### Particle number dynamics differ from model expectations

We were able to use our modified particle remineralization and sinking model to predict particle size distributions at each depth from the particle size distribution at depth one depth-bin shallower and the calculated flux attenuation between the two depths. We found that the observed particle size distributions usually varied from model expectations (Figure S10). Tautologically, at each depth, the observed size profile and the model predicted size profiles have same flux. However, the difference between the flux of observed and

predicted *small particles* (100-500), normalized to depth, serves as a valuable metric of patterns of deviations from modeled results. We call this value **OSMS** (**O**bserved **S**mall **F**lux **M**inu**s** **S**modeled **F**lux).

$$OSMS = \frac{(Small\ Flux\ Observed - Small\ Flux\ Modeled)}{\Delta Z}$$

Eqn. 3

In the above equation  $\Delta Z$  is the distance, in meters, between the current depth bin and the previous depth bin, whose particle size distribution is fed into the predictive model.

OSMS was positive between the photic zone and 500m, meaning that less small flux attenuated than would be expected from the PRISM model in this region. There was some variability in the OSMS parameter between casts. A general additive model, after factoring out the effect of depth, found that there was a statistically significant relationship between day of the cast and OSMS with highest values near day 10 of the study (which is when flux attenuation in this region was lowest) ( $p=0.01$ ) (Figure S11). However there was not a statistically significant relationship between hour of the day and OSMS.

Below 500m, OSMS was negative. There were only two casts that reached below 500m at this station, and so an analysis of the dynamics of OSMS in this region are not possible.

At P16 Station 100, OSMS was positive between the base of the photic zone and 350m and negative below 350m (Figure S9C).

## Discussion

### Diel migrators spend time in the OMZ core

Organisms of all sizes appear to migrate into the core of the OMZ. Most in the day (Figure 2A), and some at night (Figure 2B). This migratory behavior has been seen elsewhere (ref), including OMZs. One hypothesis is that the OMZ provides protection from predators of all sizes (ref). Other studies with that have characterized the diurnal and nocturnal organisms found in the OMZ, though not at this exact site. In the XXX, Mass et al saw decapods and stuff {reread that paper and find others}. At the size range seen by the 18000 kHz band, Humboldt and market squid are known to be tolerant to anoxia and to migrate into the OMZ to hunt. These small organisms likely have the greatest effect on particle transport (ref) and disaggregation (ref). Diel migration patterns are common in the ocean (ref) and zooplankton transport of particles have been indicated in other environments (ref).

The acoustic data suggests the presence of some other interesting migratory patterns. The organisms that appear between 500m and 1000m may be jellyfish (ref). The horizontal bands seen here could indicate the presence of swarms of jellyfish that migrate through the field of view of the EK60. These organisms do not seem to have much of an effect on particle size.

### Flux is lower at this site than previous measurements in the ETNP

{Unless Megan Duffy is going to have already said this somewhere}.

Flux here is lower at all depths than seen in previous measurements by traps in the OMZ (Ref). This seems reasonable, because the previous measurements were taken nearer to the coast, where surface chlorophyll is higher (Figure 1A).

## **The flux to size relationship is typical of other sites.**

The exponent of the particle size to flux relationship that we saw at our site 2.00, is of a similar magnitude to those seen by other studies that compare UVP flux to traps (Guidi et al. 2008; Kiko et al. 2020) (Guidi, Kiko). It is not identical to these measurements. This could be because these values vary between sites, or that imprecision in flux measurements leads to differences in these values between studies. Indeed, we found this value was sensitive to outlying data points.

If we left in the four traps that measured very little flux in the surface, we instead got values for this size relationship that approached zero. We feel confident excluding these traps, because it was standard for traps to under-measure flux {and maybe there were actually things observed about these}, and because we have traps at very similar depths over the same time window that provided substantially higher results. Because we have found that traps appear to under-measure flux when they fail, rather than over measure it, we have gone with the higher measurements.

## **Remineralization rates of all particles decrease in the OMZ, but disaggregation does not**

Particle size profiles, particle size distribution slopes, and estimated biovolume, averaged across all casts and smoothed, are all similar to the predictions made by Weber and Bianchi's (YYY) "Model 1". (Figure 4). This suggests that the low oxygen at this site decreases the particle remineralization rate of all particles, including small ones. It does not support the Weber-Bianchi Model 2 in which remineralization is suppressed in the OMZ, nor their model 3 in which only the very large particles' remineralization is slowed.

## **Zooplankton likely transport organic mater into the OMZ core.**

Predicted flux levels sometimes increase between 275 and 625 meters, and at all time attenuate very slowly in this region. The EK60 data suggest diel migration of organisms of all sizes to this same region. Taken together, this increase in flux concurrent diel migration, suggest transport of organic mater by zooplankton. Zooplankton may consume organic matter in the day and then release it at night (REF). That the flux varies between days suggests some day to day variability in this transport. That it is highest in the day, on average, suggests that the diel migrators may be contributing to this flux, but the fact that this diel variability is small compared to overall variability suggests that other processes may modulate this rate, and that nocturnal migrators may also play a role in carbon transport.

## **Zooplankton likely disaggregate particles in the OMZ core.**

The observation that there is more small flux that would be predicted by remineralization and sinking (positive values of OSMS) between the photic zone and 500m suggests that some process is disaggregating large particles into smaller ones. That this corresponds with the region where migratory organisms are found suggests that some of these organisms, likely zooplankton including copepods (ref), may be breaking down particles (ref). Alternatively, other processes such as spontaneous or microbial breakdown of zooplankton transported particles, or horizontal advection of water containing small particles could be responsible for this increase in small particles (ref).

Other deviations from model assumptions could also explain the increase in small particles over model predictions. For instance, if the models assumed relationship between size, flux, sinking speed and biomass are not all accurate, particle dynamics would also differ. For instance, if remineralization differed between particle types, with small particles breaking down more slowly than larger ones, perhaps because they are more labile, we might see the same kind of deviation from the model. If small particles sank more quickly for their size than expected, as has been seen elsewhere {McDonnell} (McDonnell and Buesseler 2010), a similar deviation would occur as they would have less time to remineralize per depth.

Our model also assumes a spherical particle drag profile, such that the particle sinking speed fractal dimension (*gamma*) is one less than the particle size fractal dimension (*alpha*), and that these two values sum to the particle flux fractal dimension. If any of these assumptions do not hold, or even if our calculation of the particle flux fractal dimension was in error, the magnitude of the values may differ.

Furthermore, since flux varies over time, that variability could contribute to these values, and we haven't yet deconvoluted these processes, but future models could leverage time series data like this one to incorporate multiple observed time-points into the prediction of particle size distributions at depth. One way to do this would be to use a smoothing function to interpolate particle abundances at each size, depth and times, and then to use a model in which the sinking speed of a given particle size is used to identify the relevant time-point where the abundance informs that time-point.

The opposite pattern to that seen at shallower depths occurs below 500m, with apparent flattening of the particle size distribution. This could suggest aggregation occurs here, though given the sparsity of particles, we don't see a mechanism for this process. More likely is that particles do follow PRISM like processes in this region but that likely one of our parameters are off and so disaggregation is actually higher than shown in this figure.

## Caveats

[STUB]

## Conclusions

[STUB]

## Figures

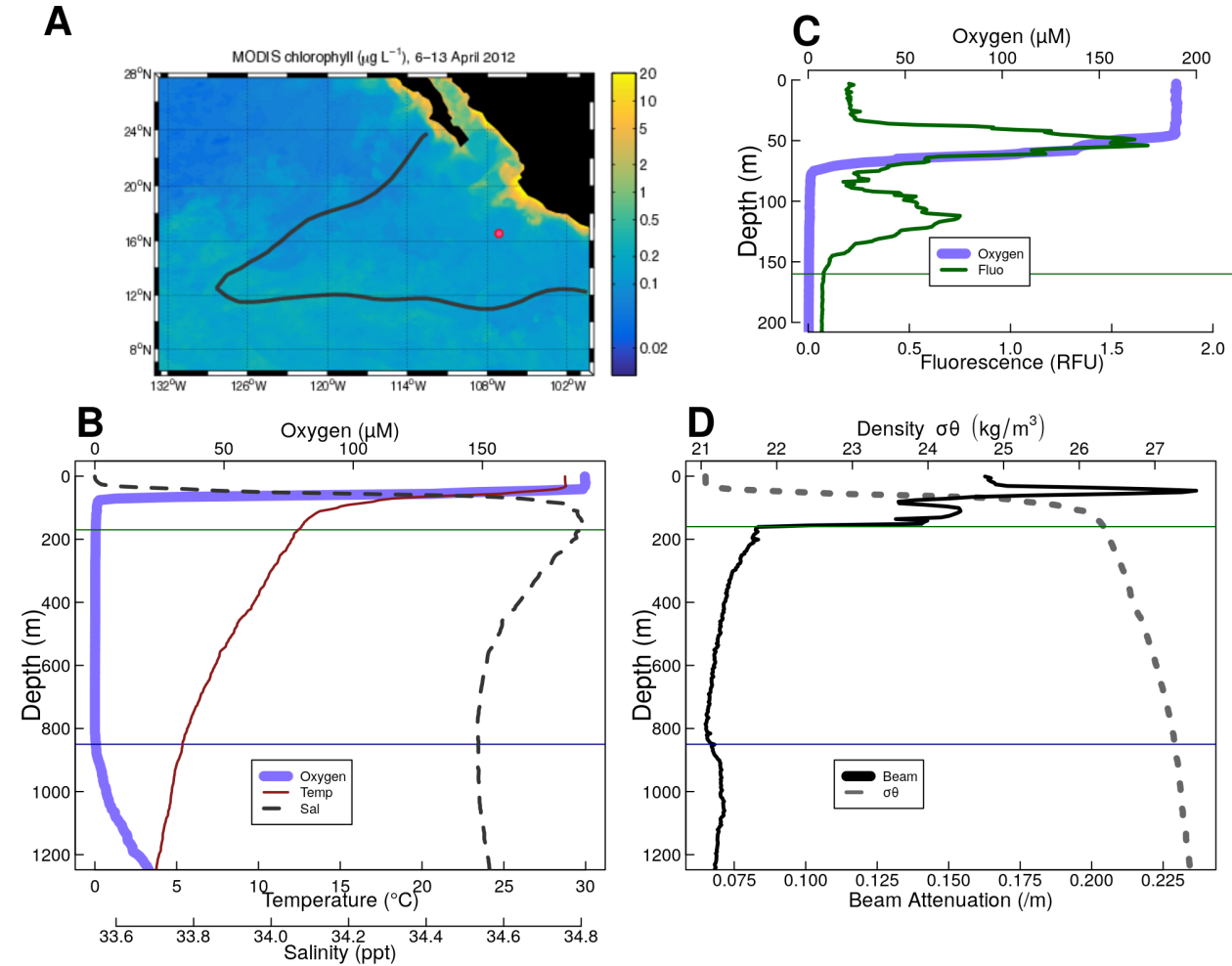


Figure 1. Overview of the geography, physics and chemistry of ETNP station P2 (A) Map of the ETNP Oxygen Minimum Zone and the location of station P2. Colors indicate chlorophyll concentrations at the surface, while the red outline signifies the region containing low oxygen. The red circle indicates the location of Station P2. (B-D) Oceanographic parameters collected from a cast at 2017-01-13 12:15 CST (local time). All profiles contain a plot of oxygen concentrations. When available, the thin horizontal green line shows the location of the base of the photic zone (160m), while the horizontal blue line shows the base of the oxycline. Figures B and D also show density (Dashed Gray Line). (B) highlights temperature and salinity. (C) fluorescence, focusing on the top 300m of the water column, and (D) beam attenuation.

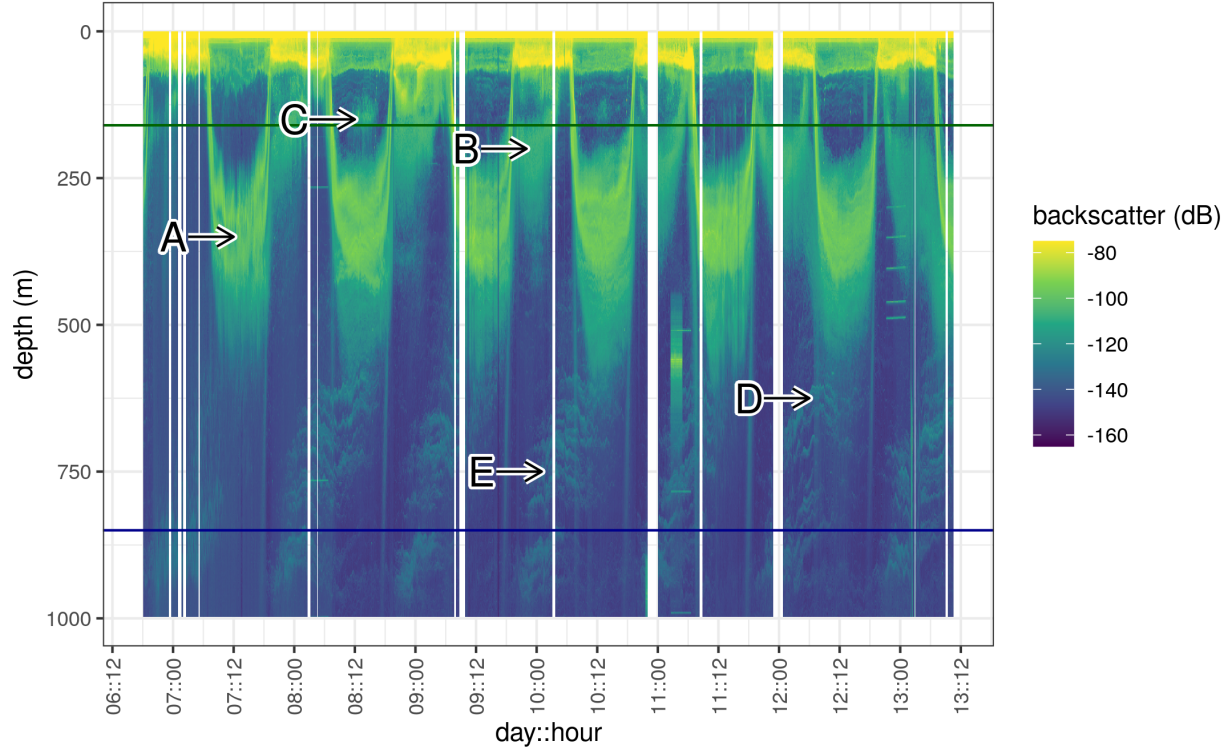


Figure 2. Acoustic data, measured by EK60, measured over the course of the experiment. Shown are data from the 18000 Hz frequency band, which have highest depth penetration, but which appear to co-occur with data from other frequency bands (see Figure SX). Values are in return signal intensity and have not been normalized to observed biomass. Several interesting patterns can be seen. **A.** Two bands of organisms can be seen leaving the surface at dawn, spending the day between 250 and 500m and returning to the surface at dusk. **B.** Another group of nocturnally migrating organisms can be seen leaving the surface at dusk, spending the night near 250m and returning at dawn. **C.** Some organisms appear at the base of the photic zone, during some, but not all mid days, and then disappear in the evening. **D.** A group of very deep migrating organisms appears to leave the surface with the diel migrants and pass all the way through the OMZ and out of the EK60's field of view. It returns at dusk. **E.** Swarms of organisms appear between 500 and 1000m disappearing later in the day. Swarms appear in the deepest layers at night and appear progressively shallower as the day progresses.

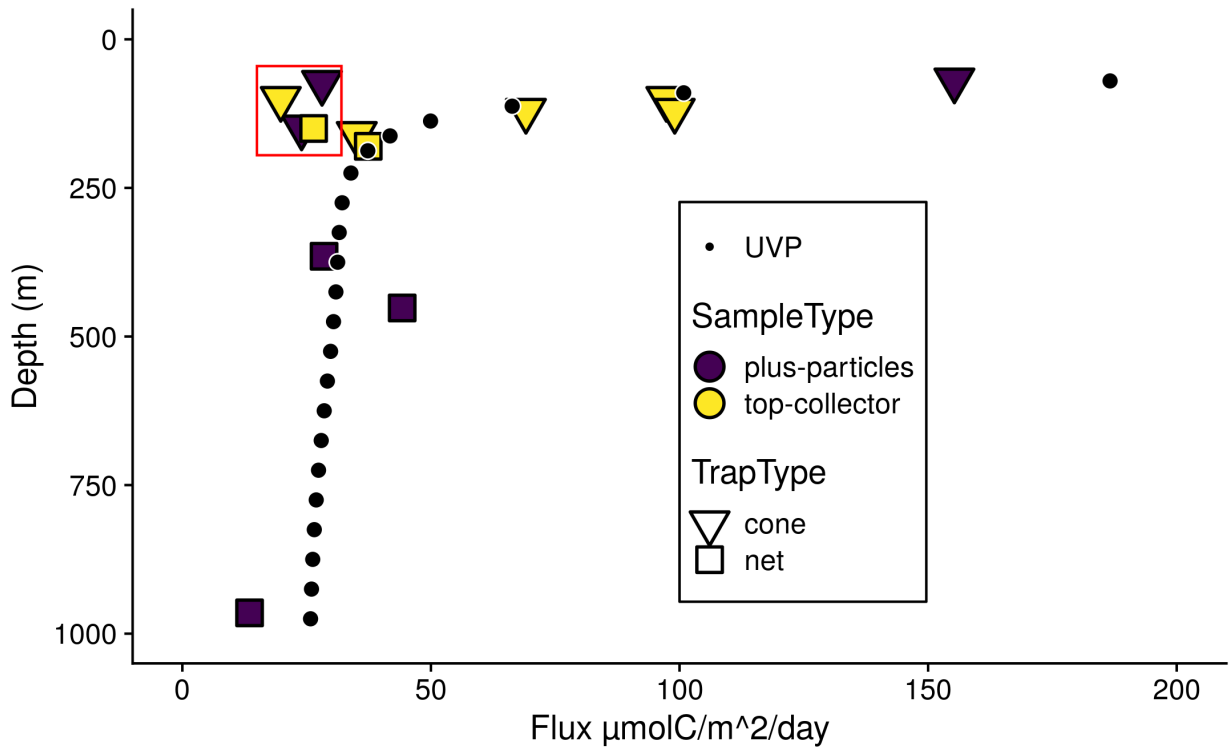


Figure 3. Particle flux, measured from sinking traps large symbols. Data from the “plus particles” and “top collector” samples from both cone and net traps were collated to generate these data. Trap types are shown by the shape and color of the large points. Superimposed are binned estimates of particle flux generated by fitting the sum of particle numbers all four profiles, binned as in Figure X, to the trap observed flux. The four points enclosed by the rectangle are unusually low compared to other traps collected at the same depth, and were therefore excluded from the fit. {Convert UVP points to a line, maybe leave points where the traps ares}

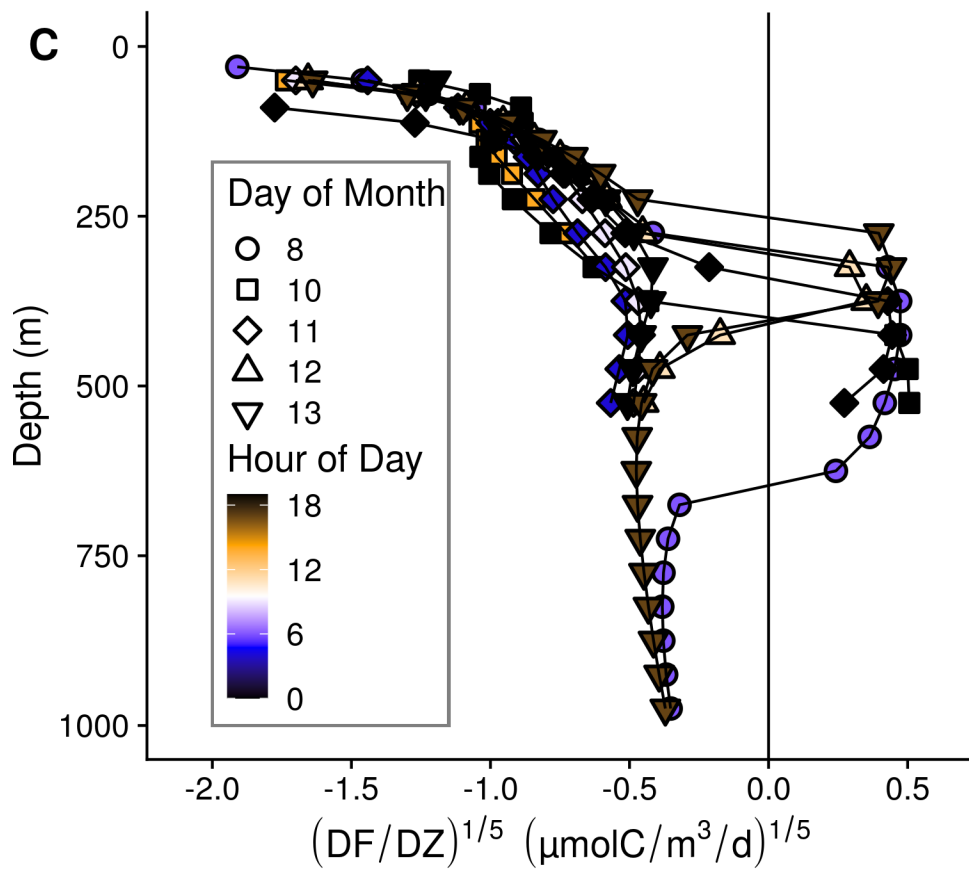
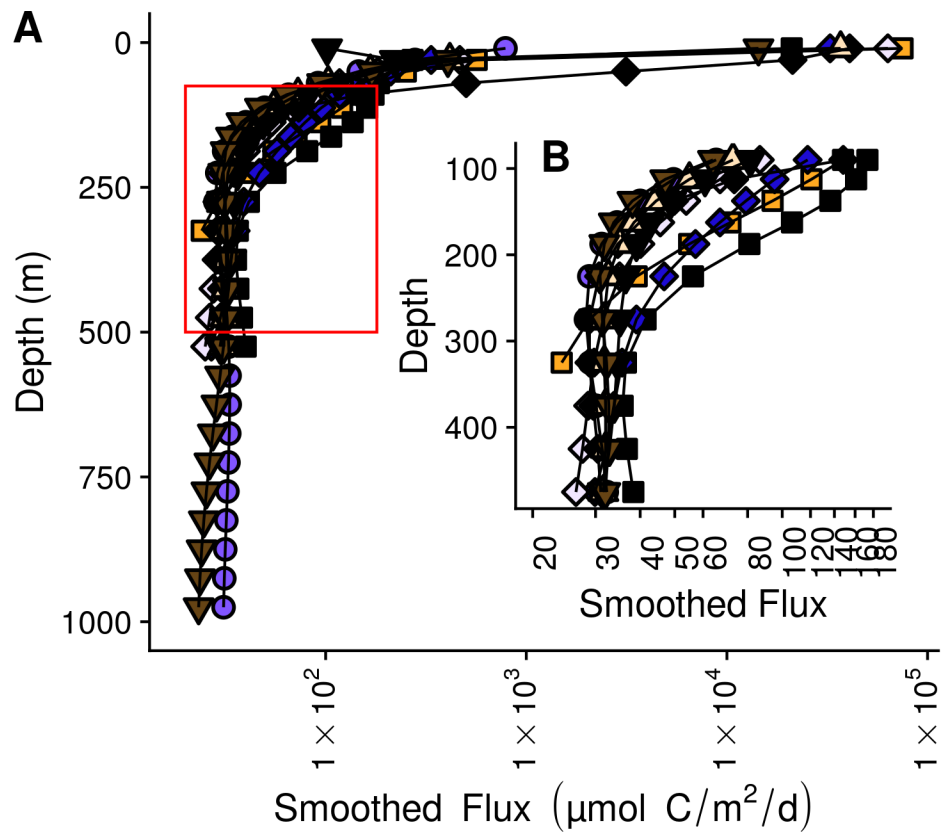


Figure 4. Within and between day variability in UVP predicted particle flux at ETNP station P2. Profiles are compared against P16 station 100, a non OMZ station at similar latitude in the tropical pacific. All profiles are depth binned with higher resolution towards the surface (methods). **(A)** Flux profiles in the top 1000m of the water column. **(B)** A more detailed depiction of the area enclosed by the rectangle in **A**. **(C)** The rate of change of flux, divided by the rate in change in depth. We show the fifth root of these values in order to highlight differences between values close to zero.

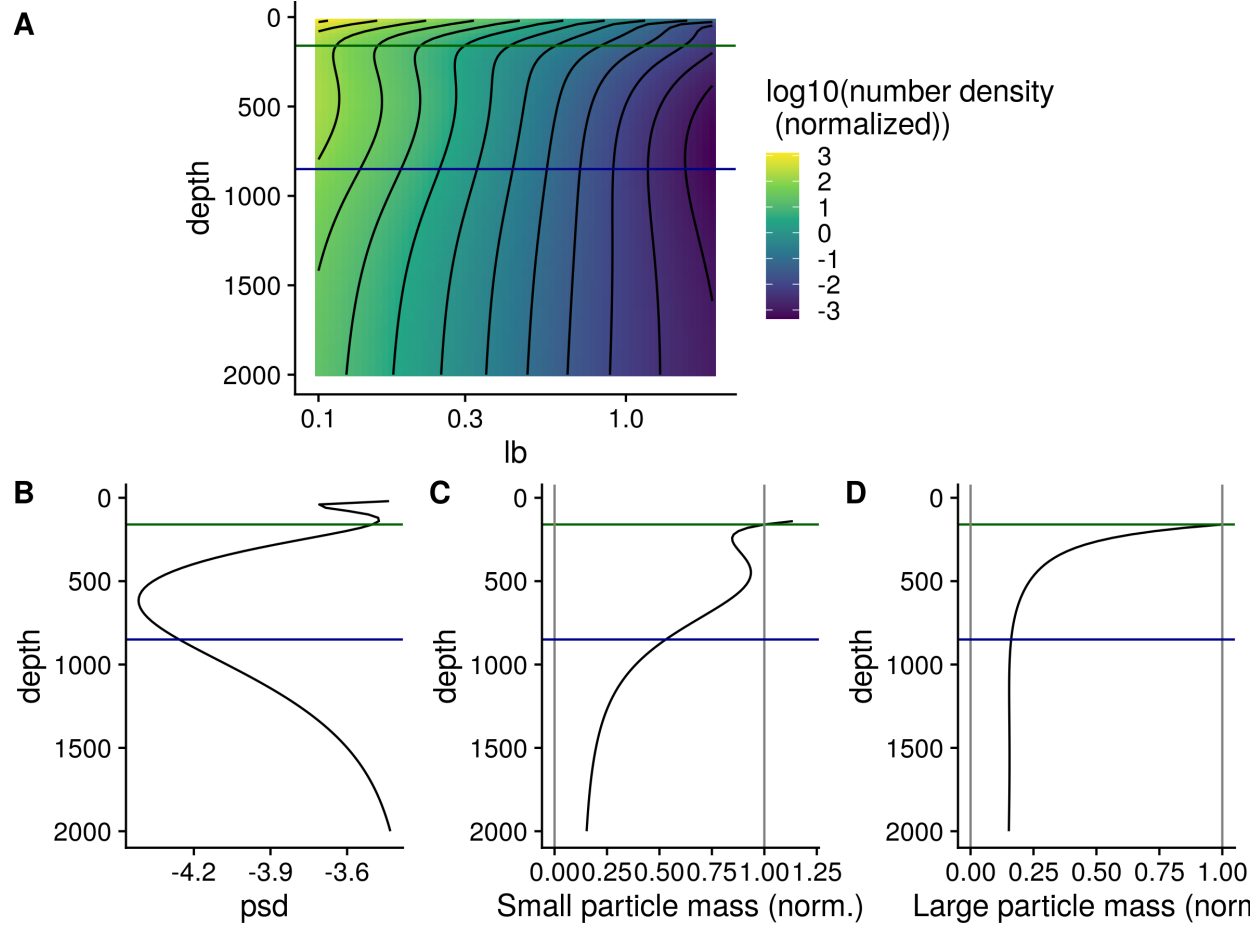


Figure 5. **(A)** GAM smoothed bin-size and volume particle numbers at each particle size class. **(B)** Particle size distributions. And estimated biomass of **(C)** Small and **(D)** Large particles.

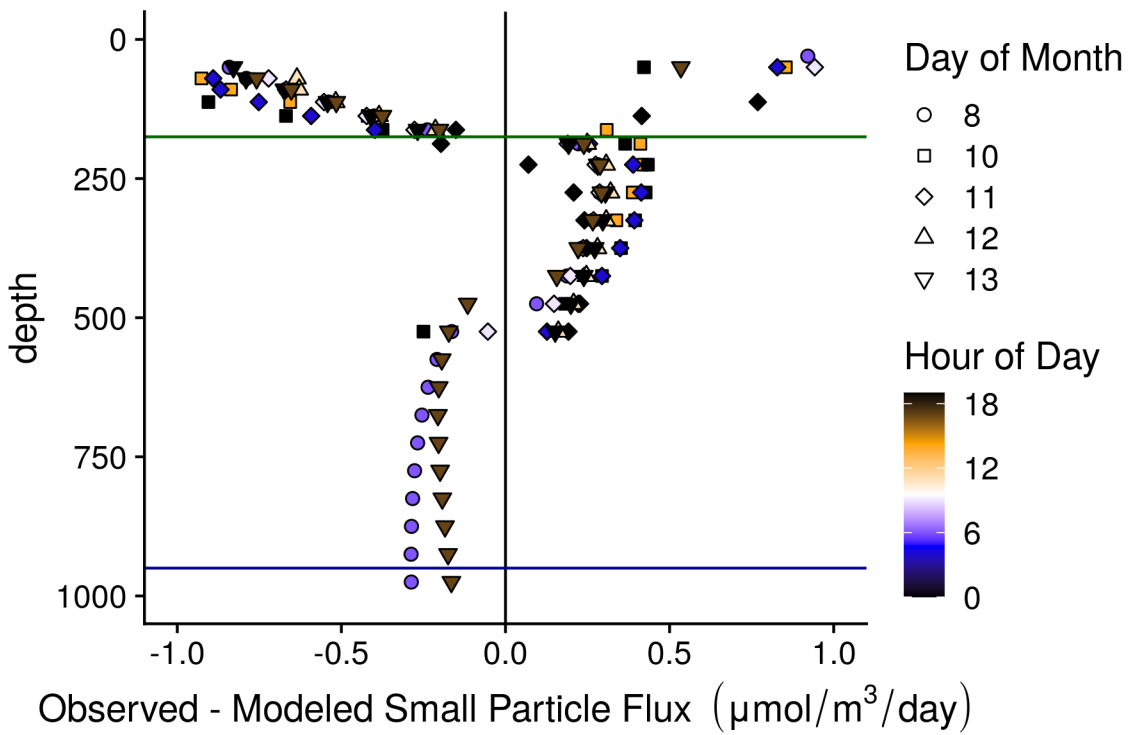


Figure 9. Quantification of non remineralization and sinking like processes. Points indicate the difference between the observed small particle flux, and the flux that would be estimated if particles from the size distribution in the depth bin above remineralized and sank only following the PRISM model. Values are normalized to the change in depth. Thus values are  $\mu\text{mol Carbon}/\text{m}^3/\text{day}$  {change to “Deviation from Model”, keep units}

## Supplemental Figs

[move to supplement]

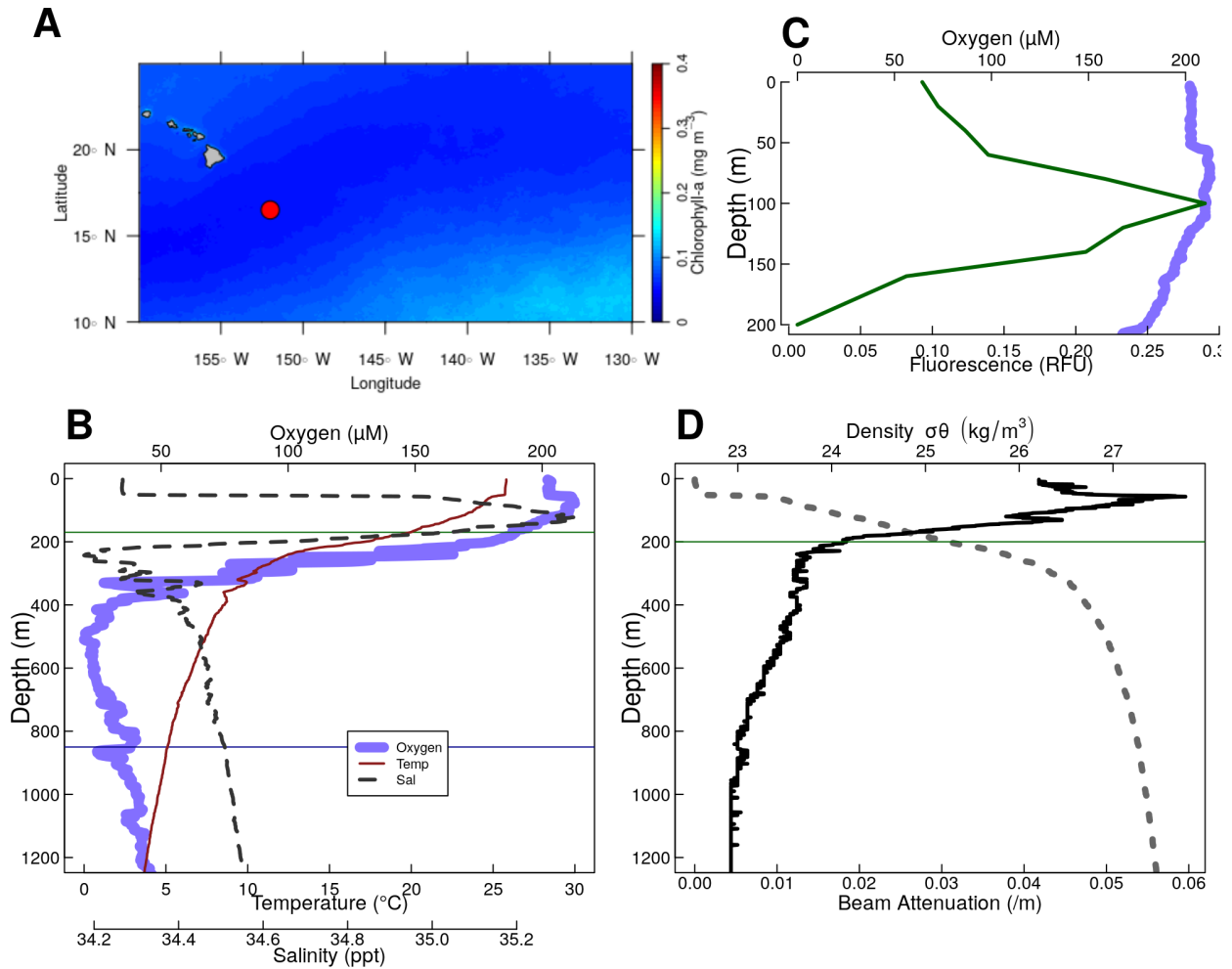


Figure S1. Physical and chemical data from P16 Station 100. Located at 16.5°N 152.0°W. (A) Map of the nearby tropical pacific station P6 Station 100. Colors indicate chlorophyll concentrations at the surface, averaged over all MODIS images. The red circle indicates the location of Station P2. (B-D) Oceanographic parameters. The thin horizontal green line shows the location of the base of the photic zone (200m m). **A** Oxygen, and fluorescence. Because the fluorometer was broken on this cruise, fluorescence data were pulled from world ocean atlas. **B** Oxygen temperature and salinity. **(C)** Beam attenuation and density, calculated from the salinity temperature and pressure data.

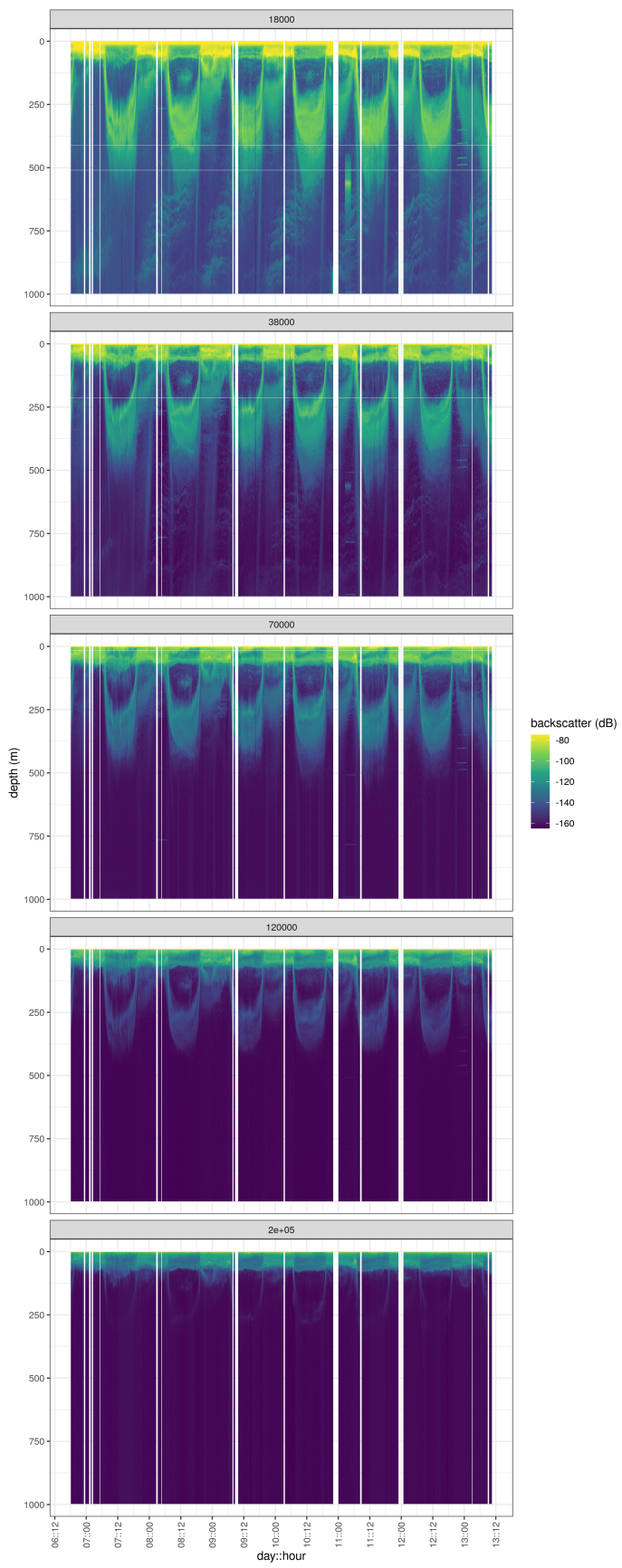


Figure S2. Acoustic data, measured by EK60, measured over the course of the experiment. Shown are data from the all frequency bands. Values are in return signal intensity and have not been normalized to observed biomass.

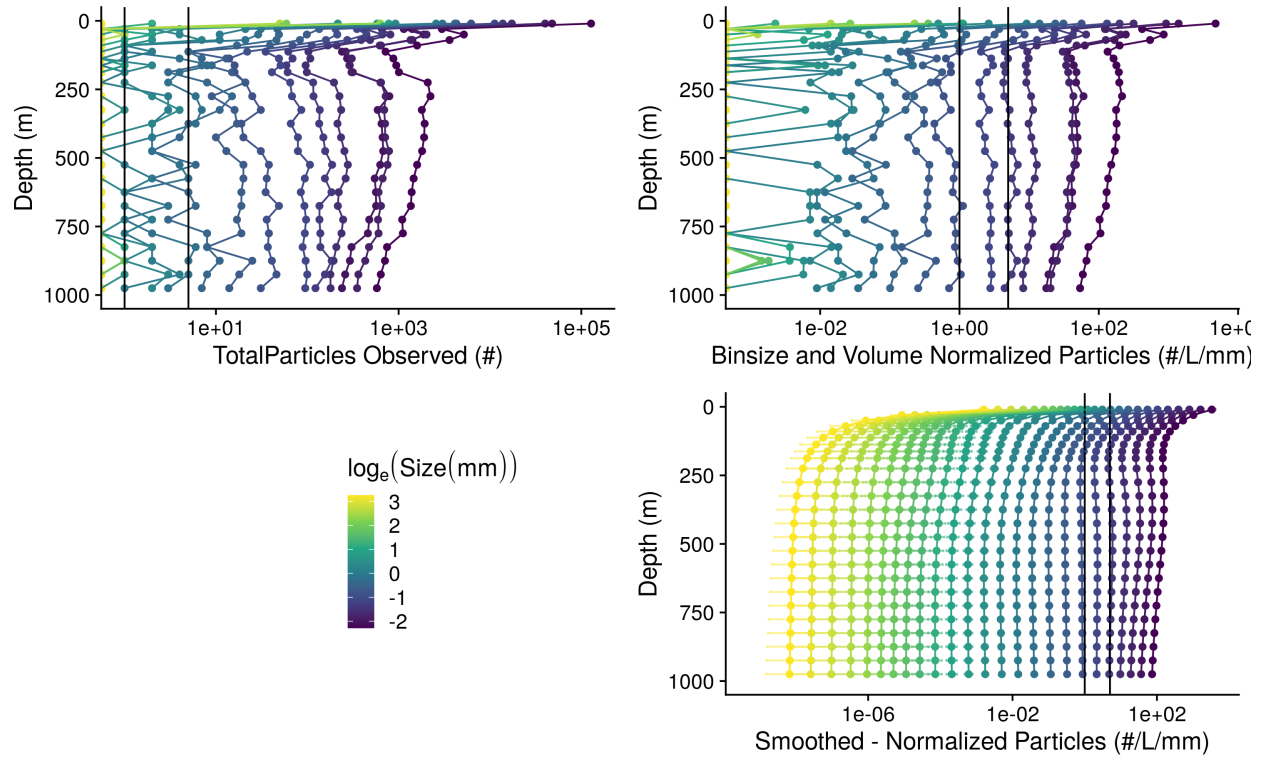


Figure S3. A profile of particle abundances at different sizes and depths. **(A)** Numbers of observed particles and **(B)** particle numbers normalized to volume sampled and particle size bin width. **(C)** Smoothed and extrapolated particle abundances, based on a negative binomial GAM that predicts particle abundance form size and depth.

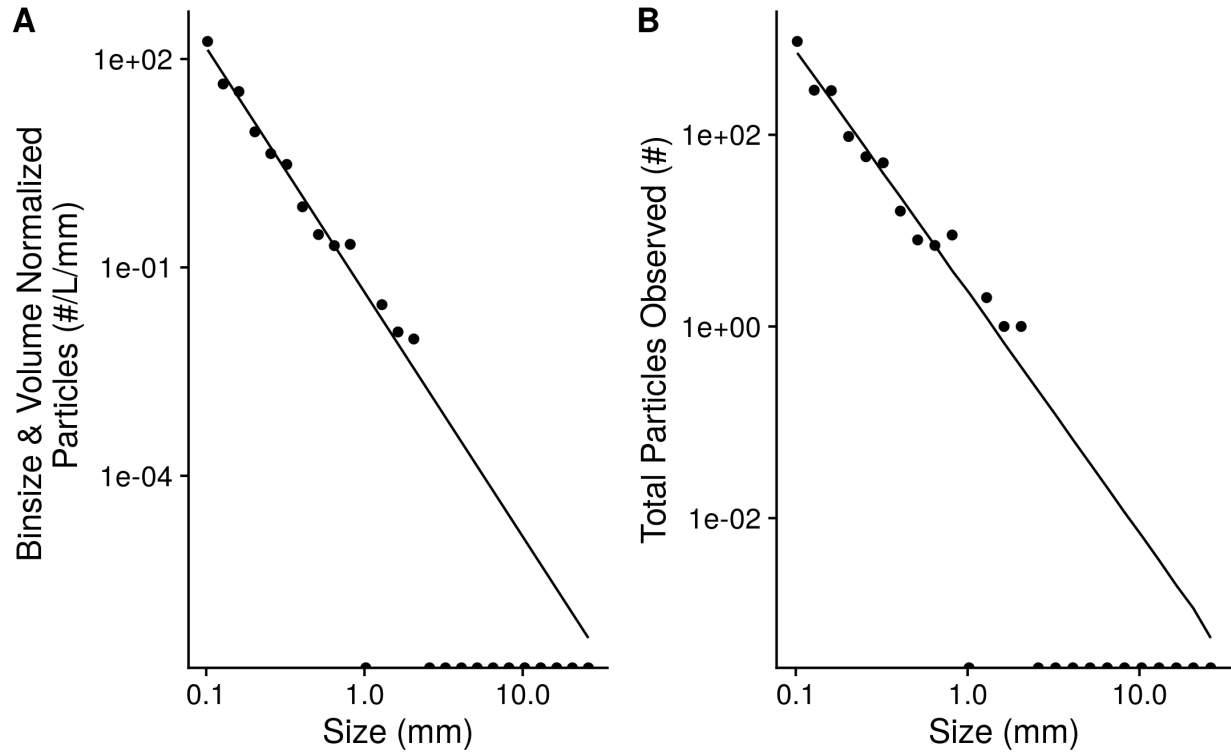


Figure S4. An example of observed particle size distribution spectra. These are depth binned data from between X and X m deep in the water column from the cast that occurred at *DATETIME* for *stn\_043*. A total volume of XXX L of water are sampled herein. Points indicate (**A**) total numbers of observed particles and (**B**) particle numbers normalized to volume sampled and particle size bin width. The line indicates the predicted best fit line of the data. The line was fit on the bin and volume normalized data by a negative-binomial general linear model. The line in panel **A** indicates predictions from this same model, re-scaled into absolute particle space.

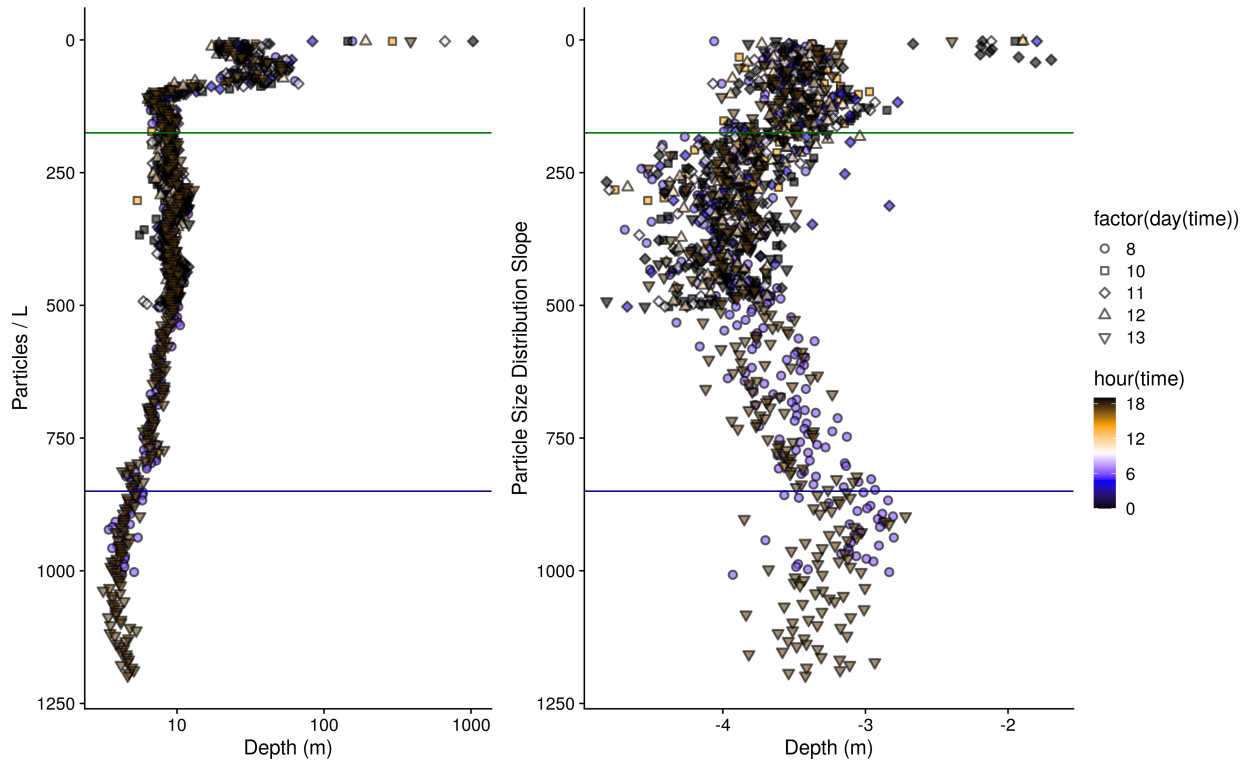


Figure S5. (A) Observed, volume normalized total particle numbers from 9 casts taken at different times of the day at ETNP station P2. (B) Calculated particle size distribution slopes of those particles. These data have not been binned by depth.

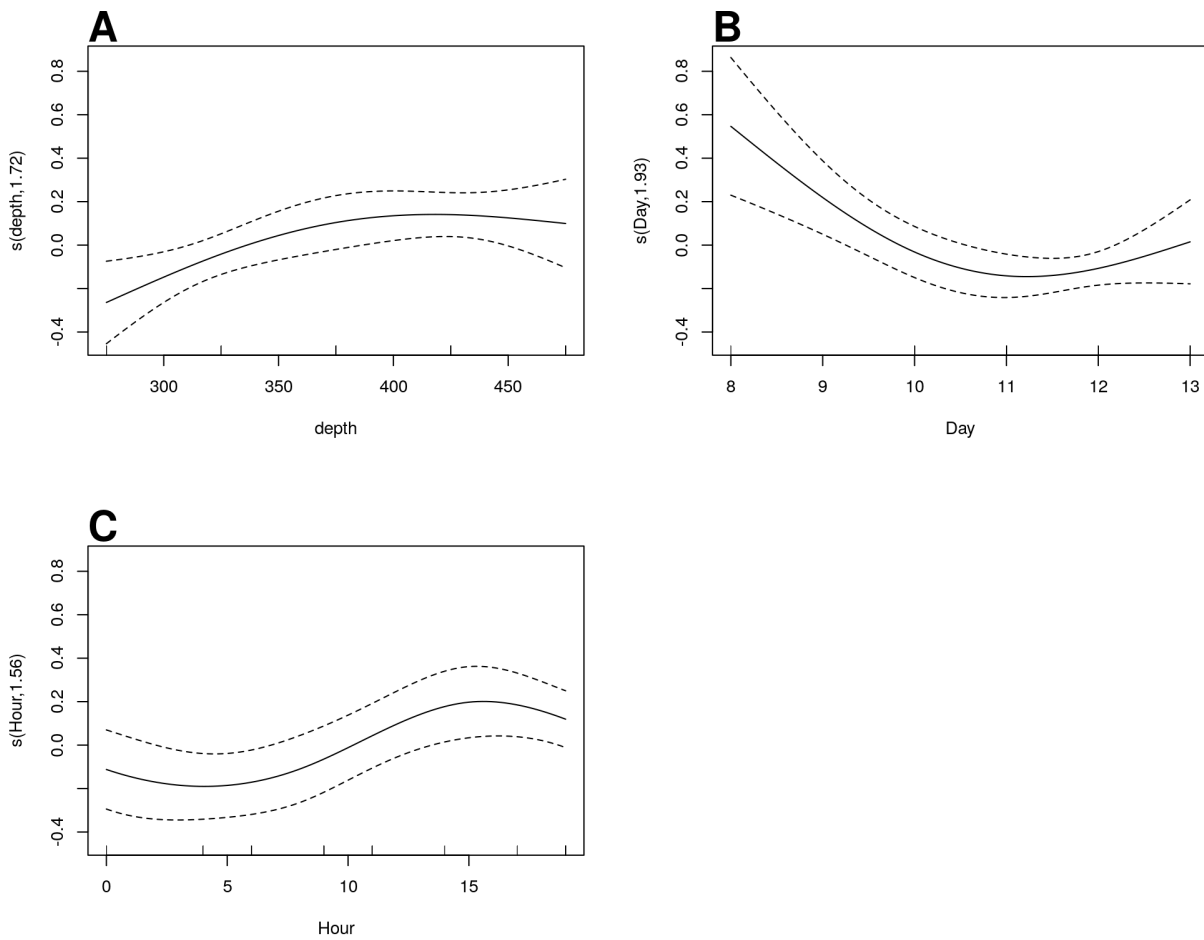


Figure S6. GAM predicted effects of **A** Depth, **B** Day of the month in January 2017, and **C** hour of the day on the fifth-root transformed, depth normalized, rate of change of flux. Y axis indicates the value of the component smooth functions effect on Flux. Positive values associate with times and regions of the water column where flux is increasing, holding other factors constant, and negative ones where it is decreasing.

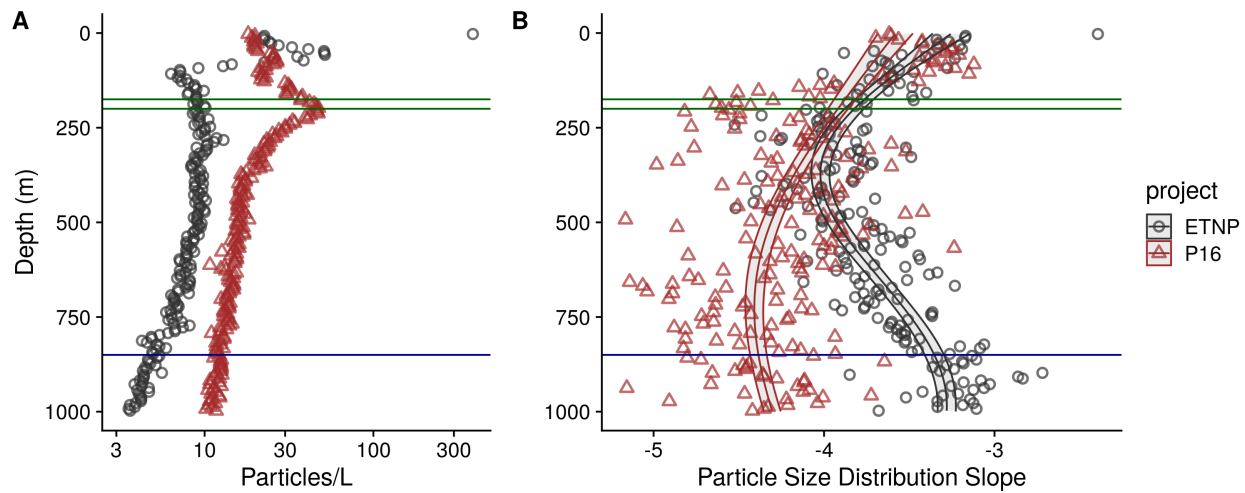


Figure S7. As above, but for the final cast taken at ETNP station P2 and the only cast collected from the

P16 transect at the station 100. P16 Station 100 was chosen because it is at a similar latitude to ETNP station P2. (A) Total particle numbers, (B) Particle size distribution. {Cut to 1000m}

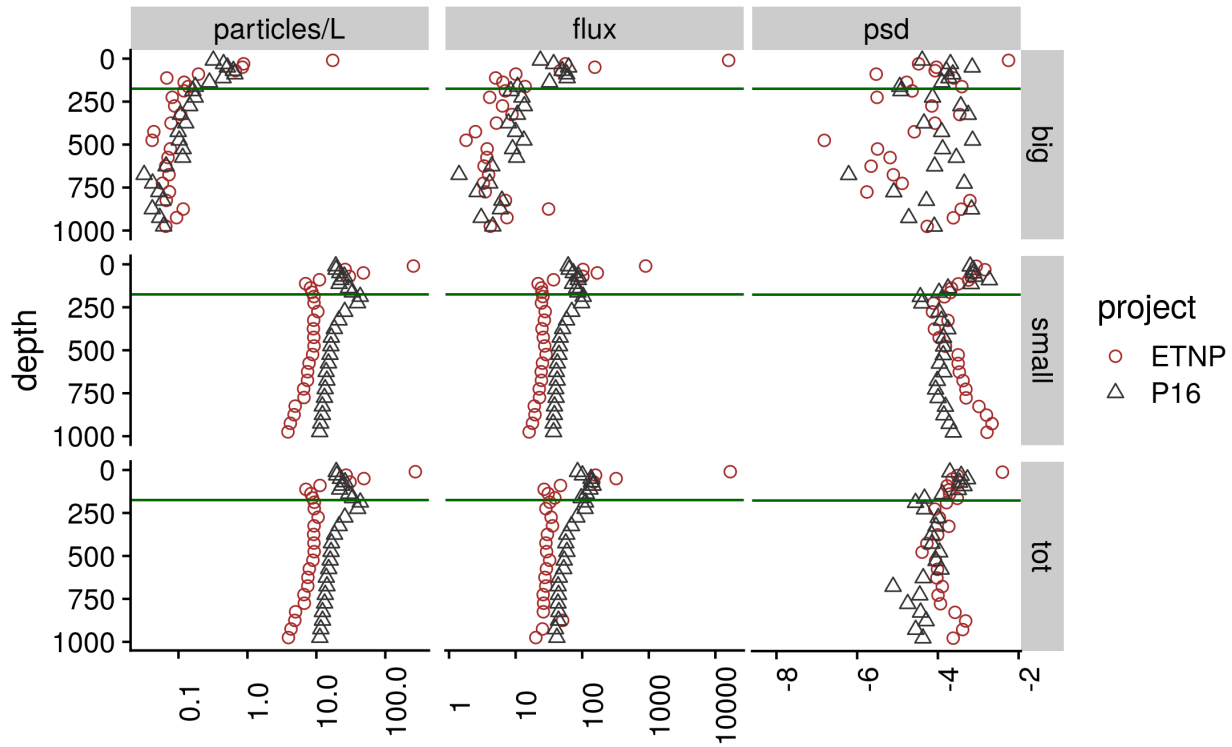


Figure S8. Depth binned particle number (volume normalized), particle size slope (PSD), and flux (estimated as in Fig. 4) for large ( $\geq 500 \mu\text{m}$ ), small ( $< 500 \mu\text{m}$ ) and total particles, at the oxic and anoxic site

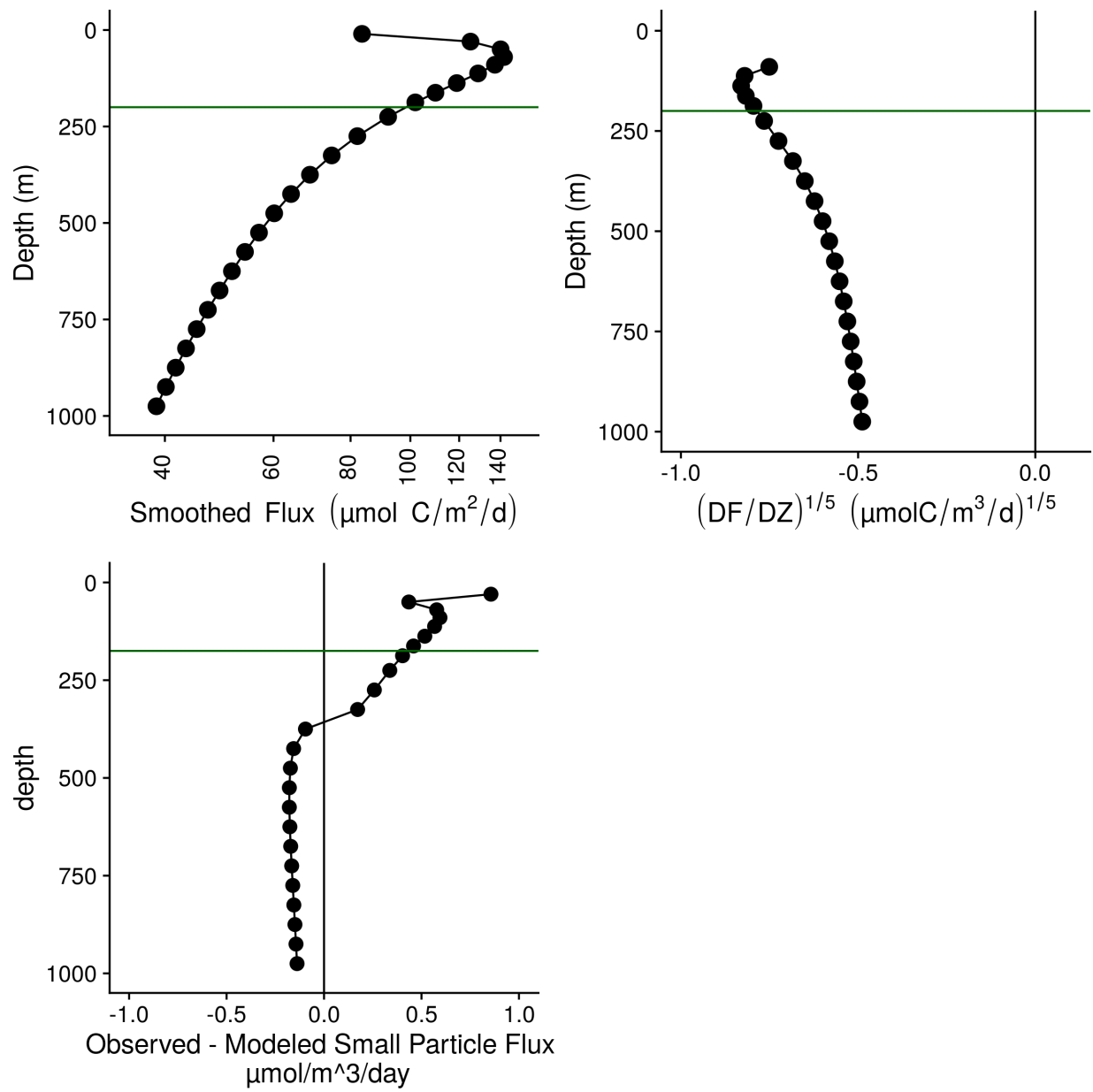


Figure S9. Flux profiles and flux attenuation at P2 Station 100. **(A)** Flux profile **(B)** Fifth-root transformed depth normalized rate of flux decrease. **(C)** Difference between observed and modeled results. Higher values suggest more disaggregation-like processes.

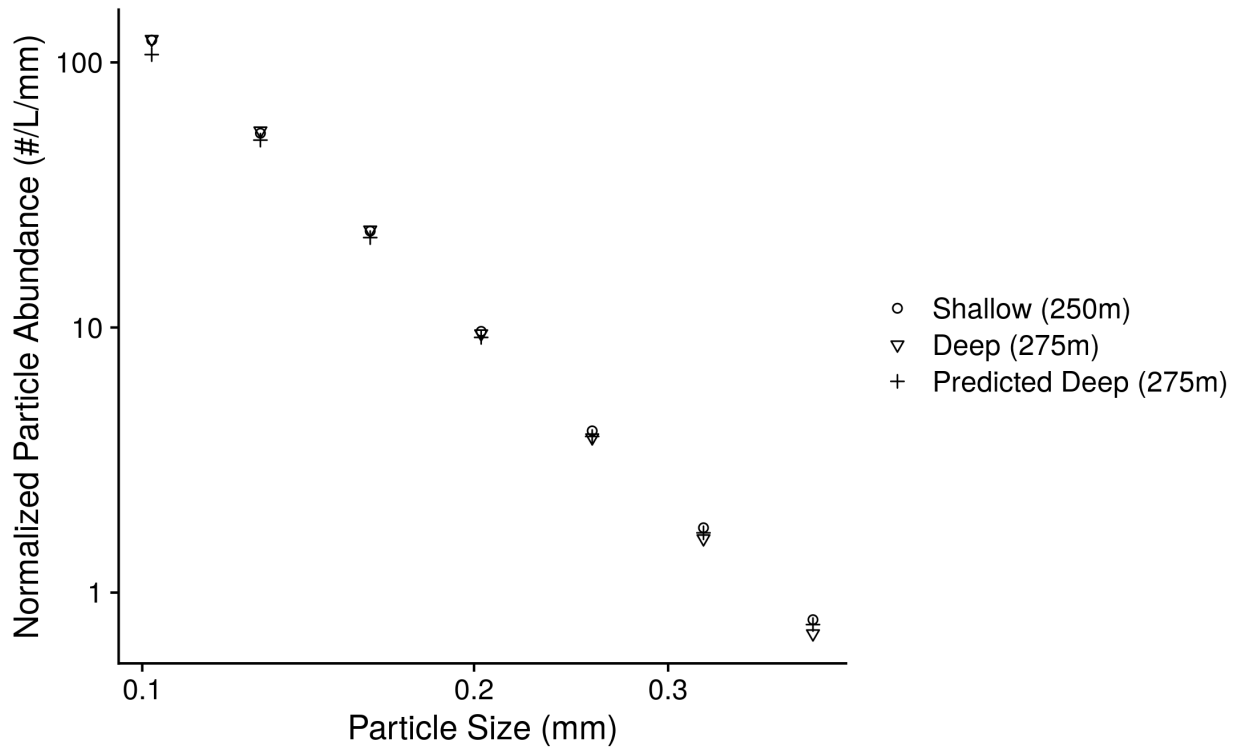


Figure S10. An example of differences between modeled and observed particle slope. Shown are profiles of particles between  $100 \mu\text{m}$  and  $500 \mu\text{m}$  than 1 mm. The particle size distribution at a shallow and deeper depth are shown. The model generates a prediction of the deep depth profile form the shallow depth profile and the flux attenuation between the two profiles. The model predicts more attenuation of the smallest particles than it actually observed.

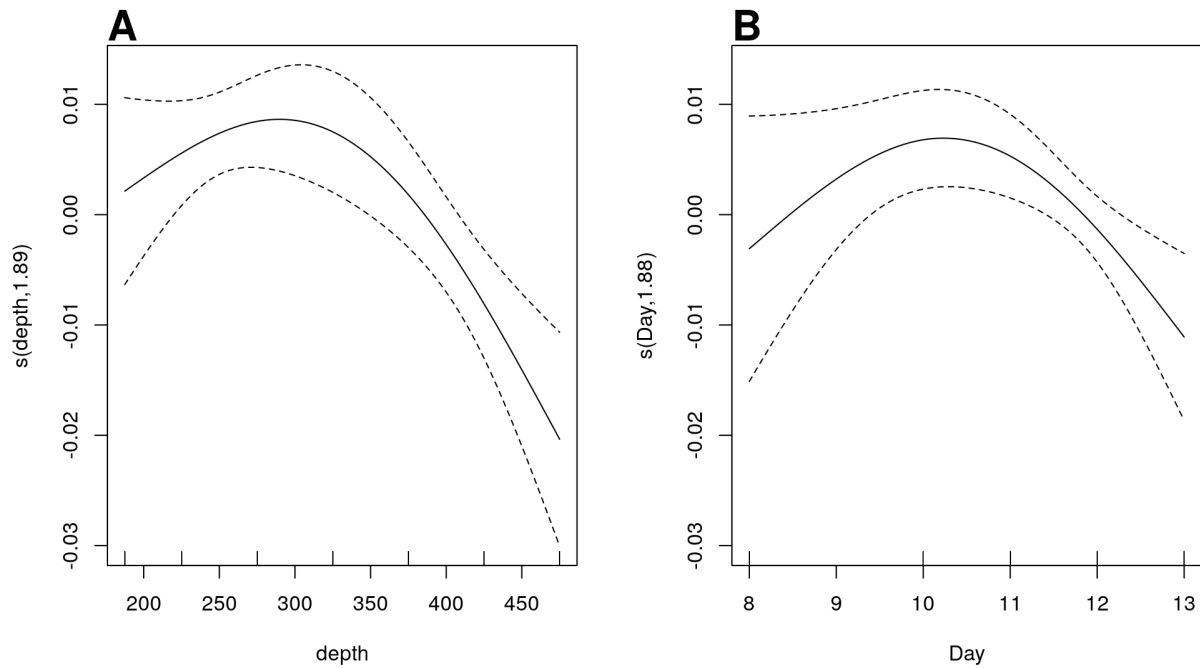


Figure S11. GAM predicted effects of **A** Depth, **B** Day of the month in January 2017 Y axis indicates the value of the component smooth functions effect on the difference between observed and modeled flux. Thus higher values correspond with greater flux of small particles than predicted by the model.

## References

- Cavan, Emma L., Stephanie A. Henson, Anna Belcher, and Richard Sanders. 2017. "Role of Zooplankton in Determining the Efficiency of the Biological Carbon Pump." *Biogeosciences* 14 (January): 177–86. <https://doi.org/10.5194/bg-14-177-2017>.
- Cram, Jacob A., Thomas Weber, Shirley W. Leung, Andrew M. P. McDonnell, Jun-Hong Liang, and Curtis Deutsch. 2018. "The Role of Particle Size, Ballast, Temperature, and Oxygen in the Sinking Flux to the Deep Sea." *Global Biogeochemical Cycles* 32 (5): 858–76. <https://doi.org/10.1029/2017GB005710>.
- DeVries, T., J.-H. Liang, and C. Deutsch. 2014. "A Mechanistic Particle Flux Model Applied to the Oceanic Phosphorus Cycle." *Biogeosciences Discuss.* 11 (3): 3653–99. <https://doi.org/10.5194/bgd-11-3653-2014>.
- Francois, Roger, Susumu Honjo, Richard Krishfield, and Steve Manganini. 2002. "Factors Controlling the Flux of Organic Carbon to the Bathypelagic Zone of the Ocean." *Global Biogeochemical Cycles* 16 (4): 34–31–34–20. <https://doi.org/10.1029/2001GB001722>.
- Gilly, William F., J. Michael Beman, Steven Y. Litvin, and Bruce H. Robison. 2013. "Oceanographic and Biological Effects of Shoaling of the Oxygen Minimum Zone." *Annual Review of Marine Science* 5 (1): 393–420. <https://doi.org/10.1146/annurev-marine-120710-100849>.
- Goldthwait, S. A., C. A. Carlson, G. K. Henderson, and A. L. Alldredge. 2005. "Effects of Physical Fragmentation on Remineralization of Marine Snow." *Marine Ecology Progress Series* 305. Inter-Research Science Center: 59–65.
- Goldthwait, Sarah, Jeannette Yen, Jason Brown, and Alice Alldredge. 2004. "Quantification of Marine Snow Fragmentation by Swimming Euphausiids." *Limnology and Oceanography* 49 (4): 940–52. <https://doi.org/10.4319/lo.2004.49.4.0940>.
- Guidi, Lionel, George A. Jackson, Lars Stemmann, Juan Carlos Miquel, Marc Picheral, and Gabriel Gorsky. 2008. "Relationship Between Particle Size Distribution and Flux in the Mesopelagic Zone." *Deep Sea Research Part I: Oceanographic Research Papers* 55 (10): 1364–74. <https://doi.org/10.1016/j.dsr.2008.05.014>.
- Keil, Richard G., Jacquelyn A. Neibauer, and Allan H. Devol. 2016. "A Multiproxy Approach to Understanding the "Enhanced" Flux of Organic Matter Through the Oxygen-Deficient Waters of the Arabian Sea." *Biogeosciences* 13 (7): 2077–92. <https://doi.org/10.5194/bg-13-2077-2016>.
- Kiko, Rainer, Peter Brandt, Svenja Christiansen, Jannik Faustmann, Iris Kriest, Elizandro Rodrigues, Florian Schütte, and Helena Hauss. 2020. "Zooplankton-Mediated Fluxes in the Eastern Tropical North Atlantic." *Frontiers in Marine Science* 7 (May). <https://doi.org/10.3389/fmars.2020.00358>.
- Kiko, R., A. Biastoch, P. Brandt, S. Cravatte, H. Hauss, R. Hummels, I. Kriest, et al. 2017. "Biological and Physical Influences on Marine Snowfall at the Equator." *Nature Geoscience* 10 (11): 852–58. <https://doi.org/10.1038/ngeo3042>.
- Kwon, Eun Young, François Primeau, and Jorge L. Sarmiento. 2009. "The Impact of Remineralization Depth on the AirSea Carbon Balance." *Nature Geoscience* 2 (9): 630–35. <https://doi.org/10.1038/ngeo612>.
- Mayor, Daniel J., Richard Sanders, Sarah L. C. Giering, and Thomas R. Anderson. 2014. "Microbial Gardening in the Ocean's Twilight Zone: Detritivorous Metazoans Benefit from Fragmenting, Rather Than Ingesting, Sinking Detritus: Fragmentation of Refractory Detritus by Zooplankton Beneath the Euphotic Zone Stimulates the Harvestable Production of Labile and Nutritious Microbial Biomass." *BioEssays: News and Reviews in Molecular, Cellular and Developmental Biology* 36 (12): 1132–7. <https://doi.org/10.1002/bies.201400100>.

- McDonnell, Andrew M. P., and Ken O. Buesseler. 2010. "Variability in the Average Sinking Velocity of Marine Particles." *Limnology and Oceanography* 55 (5): 2085–96. <https://doi.org/10.4319/lo.2010.55.5.2085>.
- Neuer, Susanne, Morten Iversen, and Gerhard Fischer. 2014. "The Ocean's Biological Carbon Pump as Part of the Global Carbon Cycle." *Limnology and Oceanography E-Lectures* 4 (4): 1–51. <https://doi.org/10.4319/lol.2014.sneuer.miversen.gfischer.9>.
- Picheral, Marc, Lionel Guidi, Lars Stemmann, David M. Karl, Ghislaine Iddaoud, and Gabriel Gorsky. 2010. "The Underwater Vision Profiler 5: An Advanced Instrument for High Spatial Resolution Studies of Particle Size Spectra and Zooplankton." *Limnology and Oceanography: Methods* 8 (9): 462–73. <https://doi.org/10.4319/lom.2010.8.462>.
- Steinberg, Deborah K., and Michael R. Landry. 2017. "Zooplankton and the Ocean Carbon Cycle." *Annual Review of Marine Science* 9: 413–44. <https://doi.org/10.1146/annurev-marine-010814-015924>.
- Steinberg, Deborah K., Benjamin A. S. Van Mooy, Ken O. Buesseler, Philip W. Boyd, Toru Kobari, and David M. Karl. 2008. "Bacterial Vs. Zooplankton Control of Sinking Particle Flux in the Ocean's Twilight Zone." *Limnology and Oceanography* 53 (4): 1327–38. <https://doi.org/10.2307/40058255>.
- Stramma, Lothar, Gregory C. Johnson, Janet Sprintall, and Volker Mohrholz. 2008. "Expanding Oxygen-Minimum Zones in the Tropical Oceans." *Science* 320 (5876): 655–58. <https://doi.org/10.1126/science.1153847>.
- Turner, Jefferson T. 2015. "Zooplankton Fecal Pellets, Marine Snow, Phytodetritus and the Ocean's Biological Pump." *Progress in Oceanography* 130 (January): 205–48. <https://doi.org/10.1016/j.pocean.2014.08.005>.
- Van Mooy, Benjamin A. S, Richard G Keil, and Allan H Devol. 2002. "Impact of Suboxia on Sinking Particulate Organic Carbon: Enhanced Carbon Flux and Preferential Degradation of Amino Acids via Denitrification." *Geochimica et Cosmochimica Acta* 66 (3): 457–65. [https://doi.org/10.1016/S0016-7037\(01\)00787-6](https://doi.org/10.1016/S0016-7037(01)00787-6).
- Weber, Thomas, and Daniele Bianchi. 2020. "Efficient Particle Transfer to Depth in Oxygen Minimum Zones of the Pacific and Indian Oceans." *Frontiers in Earth Science* 8. Frontiers. <https://doi.org/10.3389/feart.2020.00376>.